Journal of Computers Vol. 30 No. 4, 2019, pp. 90-105
doi:10.3966/199115992019083004008

Electrostatic Tactile System Analyzing and Modelling

Xue-Zhi Yan[1*], Rui-Ge Li[1], Xiao-Ying Sun[1]

[1] Department of Communication Engineering, Jilin University, Renmin Street, Changchun, China
yanxz@jlu.edu.cn, lirg15@mails.jlu.edu.cn, sunxy@jlu.edu.cn

Received 20 December 2017; Revised 14 May 2018; Accepted 4 July 2018

Abstract. An effective system equivalent circuit model plays an important role in understanding system characteristics and improving system performance. However, most existing studies provided only final models, it's unclear what factors and how these factors affect electrostatic tactile system exactly. Based on the custom-designed electrostatic tactile device, we analyzed completely the effects of ground connection method, human body grounding position, human impedance and insulator capacitance on system output performance in this paper. Analysis results show the output voltage under direct connection is six times larger than under nature connection, proving the necessity of direct ground connection. Furthermore, we also proved the negligible effects of human body grounding position and human impedance. Finally, we show larger permittivity and smaller thickness of insulator may cause better system performance. Based on these findings, we established a practical equivalent circuit model and analyzed system frequency characteristics and waveform characteristics.

Keywords: circuit parameters analyzing, electrostatic tactile system, equivalent model, modeling

1 Introduction

Fuelled by the popularity of touchscreen products in both research and end-user communities, technology of human computer interaction has been rapidly developing and widely used to replace keyboard and mouse operations in many applications [1]. The simply use of vision and auditory limits the applications of touchscreen products in noisy and visual disorder environments [2]. Therefore, tactile representation which improves the sense of immersion has been paid more attentions. Tactile representation systems can be divided into four kinds: vibration-stimulated, pressure-stimulated, squeeze film-based and electrostatic-based representation system. The vibration-stimulated [3-4] and pressure-stimulated [5-6] representation systems have many problems such as too strong sense of vibration, gas leakage and so on, while the squeeze film-based systems [7-9] cause great power consumption. Therefore, more researchers have focused on the electrostatic-based representation system.

Electrostatic device is probably most promising in all kinds of tactile devices because of several compelling properties. It is fast, low-powered, low-noise, and easy to integrate with touchscreen to be used in a wide range of interaction scenarios and applications. Most previous work on electrostatic tactile system falls into two categories: One is the hardware devices [1, 10-12], the other is feature extraction or rendering algorithms for visual contents [13-16]. However, problems of electrostatic tactile system analyzing and modeling, which is of great importance in understanding system characteristics and guiding design of the future applications, have not been fully studied.

Equivalent physical model of the system is the powerful tool for analyzing complex system. It helps researchers convert many physical features, processes and physical quantities that are difficult to observe and measure directly to some indirect observable and measured variables. The internal structure and the corresponding characteristics of the mobile terminal can be analyzed by establishing the equivalent physical model of the electrostatic tactile representation terminal. Recently, researchers from the Northwestern University and the University Lille1 have made some efforts in Electrostatic tactile modeling and analyzing [17-20]. They gave the equivalent models directly and used different ways to

* Corresponding Author

analyze the temporal evolution and frequency dependence of the input signals. However, these studies didn't analyze the possible factors which will affect the system. These factors that are not explicitly studied may affect modeling and analyzing of electrostatic tactile system, impeding the practical application of Electrostatic tactile products.

When considering possible influencing factors, we focus on ground connection method, human impedance and different human body grounding position which are important for electrostatic tactile system modeling but not been fully studied. Although human bodies provide a natural link to the ground, creating a direct ground connection is proved necessary in the practical usage. It not only allows the system and its associated circuits to operate reliably and precisely, but also increases tactile sensation intensity significantly [1]. The effect of ground connection method which is worth studying deeply is proved from experiments but not in theory. In addition, different users have different human impedance characteristics including skin impedance and human interior impedance [21]. the feasibility of electrostatic tactile system to human impedance characteristics determined target users and applied ranges of electrostatic tactile representation products, which must be considered in electrostatic tactile system modeling and analyzing. For example, if skin impedance has a great effect on the usage of the electrostatic device, researchers must take the effective grounding methods into account, which may increase productive costs and limit applied scopes of the device to a large extent. If the system has a bad feasibility to human interior impedance, it may not be suitable for the overweight with larger interior impedance or the overthin with smaller interior impedance. Beyond that, the selection criteria of insulator capacitance is also important for Electrostatic tactile devices manufacture and tactile performance improvement. However, the problems of these factors which are of great importance in designing and using electrostatic devices are not been fully studied.

With the custom-designed Electrostatic tactile device, we explore the effect of ground connection method, human impedance, human body grounding position and insulator capacitance on system performance. Based on above results, we establish an equivalent model of electrostatic tactile system and analyze system frequency characteristics and waveform characteristic through the system function. The contributions are summarized as:

(1) We show that output voltage under direct connection is six times larger than that under nature connection, whereas human body grounding position has no significant difference and can be chosen freely, proving the necessity of direct ground connection and negligible effect of human body grounding position;

(2) We show the negligible effect of human impedance and prove that larger permittivity and smaller thickness of insulator may cause better system performance, providing guidelines of the electrostatic devices manufacture and new materials development;

(3) We show the system frequency characteristics and waveform characteristics and then provide guidance for the usage of applied signals based on the presented model, which is of great importance in designing applications of electrostatic tactile system.

2 Backgound

In this section, we focus on the research status of electrostatic tactile system and then introduce our electrostatic tactile device. Finally, we study existing equivalent models of electrostatic tactile system to show the research advancements and existing problems.

2.1 Electrostatic Tactile System

When the dry finger sliding on a charged conductor covered with insulating materials, the charged conductor and conducting tissues under the finger skin form a condenser, of which the insulator and the stratum corneum of dry outer skin are dielectric [22]. As the principle of electrostatic tactile system shown in Fig. 1, an intermittent attraction force develops between the finger and conductor when alternating voltage is applied to the conductor.

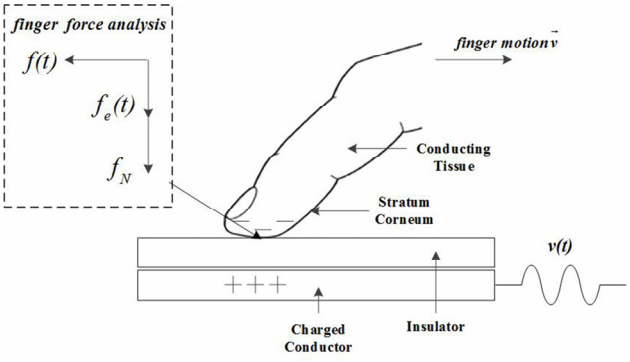

Fig. 1. Principle of electrostatic tactile representation

Whereas the electrostatic attraction is too weak to be perceived when the finger is static, it cause the change of friction which is easy to be detected when sliding finger. It is through adjusting friction between the finger and the panel that electrostatic tactile devices represent many kinds of tactile feelings. The electrostatic attraction $f_e(t)$ and friction $f(t)$ can be expressed as (1) and (2), where f_N is finger pressure, μ is friction coefficient, ε_0 is vacuum permittivity, A is the finger area in contact with the insulator, $v(t)$ is the transient voltage applied to the conductor, T_i and T_{sc} are respectively the thicknesses of insulator and stratum corneum, ε_i and ε_{sc} are respectively the relative permittivity of insulator and stratum corneum [1].

$$f_e(t) = \frac{\varepsilon_0 A[v(t)]^2}{2(\frac{T_i}{\varepsilon_i} + \frac{T_{sc}}{\varepsilon_{sc}})(T_i + T_{sc})} \tag{1}$$

$$f(t) = \mu(f_e(t) + f_N) \tag{2}$$

Many researchers had made achievements in the field of Electrostatic tactile devices, but these devices are difficult to integrate with touchscreens in early stage. In 1970, Strong and Troxel first used the Electrostatic tactile principle in practical and constructed an electrotactile device [22]. In 2006, a new display developed by Yamamoto A et al. represented tactile feelings in a non-transparent telepresentation system through a thin conductive film slider with stator electrodes [11]. Recently, researchers have overcome the imperfection gradually and applied the technology to existing touchscreen products. Based on the electrostatic stimulation technology via capacitive coupling, Senseg Company developed a novel haptic display (E-Sense screen) to add Electrostatic tactile easily in existing touchscreens [1]. Similarly, Disney Research developed TeslaTouch to provide a wide range of tactile feedback sensations. They also applied Electrostatic tactile technology for the visually impaired to help them reading and walking [23, 24]. These studies make important contributions to the hardware platform but still have rooms for providing efficient tactile experience through modeling and analyzing of the electrostatic system.

2.2 Electrosvibration System Equivalent Model

The Northwestern University and the university Lille1 have done many relevant works and put some equivalent physical model of electrosvibration system. In 2012, Meyer DJ discussed the underlying physics of electrostatic attraction and presented a mathematical model for electrostatic force on a human finger [19]. Based on above studies, they established an electrostatic tactile system equivalent model and proved the amplitude effectiveness of the model with their measurement platform [20]. Giraud F et al. took the resonant behavior of the experimental test bench into account and established models of electrostatic tactile system and squeeze-film system [21]. However, their studies didn't consider the charge leakage phenomenon of the human finger and failed to prove the frequency effectiveness. Furthermore, Vezzoli E et al. proposed an improvement equivalent model with a focus on the temporal evolution and frequency dependence of the signal [22]. They also applied their models to the joint use of Electrostatic tactile devices and squeeze-file devices [25-26]. Recently, Kim et al. suggested a method based on current control to solve the nonuniform intensity problem [27]. Yasemin V et al. used the presented model to explore waveform effectiveness and showed that users were more sensitive to square

wave in low frequency [28]. Although the amplitude characteristic and frequency characteristic were explored in above studies based on their presented models, the models were given directly without discussing the influencing factors and practical application methods. Why the models were built like these, or what factors will affect the model in what way? All these questions about electrostatic tactile system modeling which are of great importance in understanding and practically using the electrostatic devices have not been fully studied.

2.3 Bioelectric Properties of Human Finger Skin

The body is composed of a large number of tissue cells with very complex structure. The skin is the body's tactile interface with complex structure and fine tactile resolution. The skin can be divided into four parts: the Stratum Corneum, the Epidermis, the Dermis and the Hypodermis, the Stratum Corneum among that is the outermost structure of the skin with a large number of dead cells.

In the power state, the front and back of the Stratum Corneum included positive and negative charges to constitute a capacitor. The Stratum Corneum itself of which the conductivity is about 100-1000kΩ·m was hard to conduct, so it was seen as a larger resistance and act as intermediate medium of the capacitor. However, the Stratum Corneum had sweat glands and other pore structures, the sweat of which consists of free charges, so it was conducted and equivalent as parallel structure of capacitance and resistance. In summary, Stratum Corneum can be equivalent to the form of resistance and capacitance in parallel, as shown in Fig. 2, where R_{sc} and C_{sc} were respectively the equivalent resistance and capacitance of the Stratum Corneum.

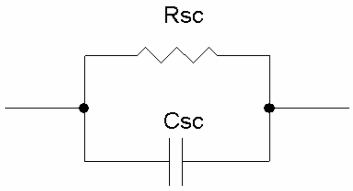

Fig. 2. The equivalent physical model of stratum corneum

The thickness and relative permittivity of human stratum corneum affect the skin capacitance greatly. We found that the thickness of stratum corneum is related to many factors. Researchers from University of Marburg measured the thickness of the stratum corneum through optical coherence tomography and then obtained the average thickness of the stratum corneum through the analysis of data on 105 experimenters [29]. The dielectric constant of the stratum corneum decreases at first and then increases exponentially towards the deeper tissues, while the resistivity decreases in an exponential fashion [30].

3 Electrostatic Tactile Parameter Analysis

3.1 Ground Connection Methods

In this subsection, electrostatic tactile system under direct ground connection and nature ground connection are first taken into account as shown in Fig. 2, where we equivalent intrinsic structure of skin stratum corneum to a parallel connection of resistivity and permittivity [31].

Due to the charge leakage phenomenon, some lost charges gather on the surface of the insulator as free charges when energizing, so the insulator is equivalent to an individual capacitance rather than form a capacitance together with skin stratum corneum. When the device grounds directly, there must be one hand (or a finger) touched the ground point and another hand slid screen directly. Therefore, two finger skin stratum corneum and human impedance between them are considered under direct ground connection shown in Fig. 2(a). Conversely, nature ground connection relies shoes or chair legs connected directly with the earth to ground and form a loop, as shown in Fig. 2(b). In addition, the electrostatic tactile system works at low frequency in most cases because the human sensitivity frequency is in the range of 10Hz-1000Hz, so the effect of stray capacitances whose capacitance characteristics are appeared only at high frequency are ignored.

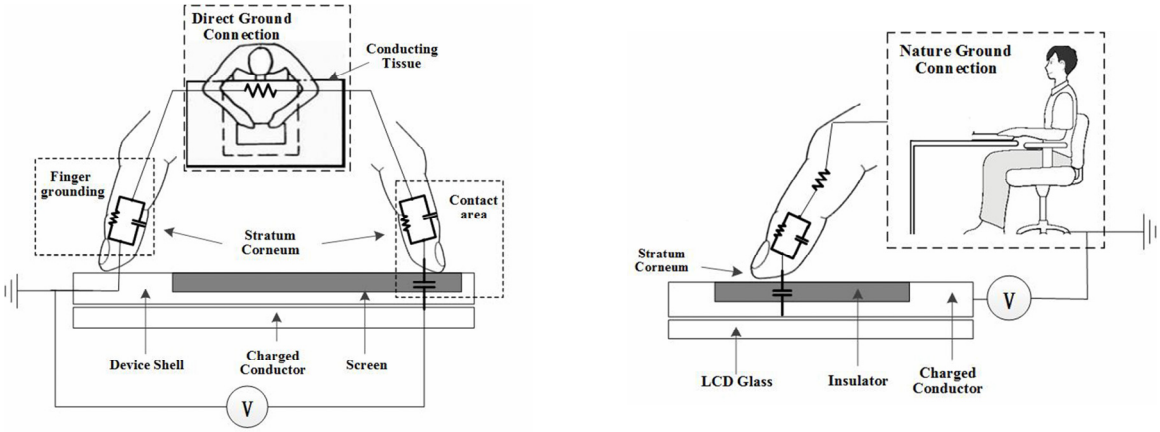

(a) under direct ground connection (b) under nature ground connection

Fig. 2. Actual usage of electrostatic device

The equivalent circuit models are shown in Fig. 3, where R_{sc1}, C_{sc1} and R_{sc2}, C_{sc2} are resistances and capacitances of fingers' stratum corneum respectively sliding on the touchscreen and touching direct ground point, R_H is interior resistance between the two fingers (hereinafter known as 'human impedance'), C_i is the capacitance of the insulator, V is the applied voltage, V_{sc1} and V_{sc1} are output voltages acting on the finger filtered by the human skin respectively under direct ground connection and nature ground connection (hereinafter known as 'effective voltage'), Z is environmental impedance such as shoes or chair legs. Whereas some researchers used voltage between the conductor and conducting tissue or voltage difference across the air gap to generate electrostatic force [32], we think that the electrostatic force occur at the inner boundary of the stratum corneum as the mechanoreceptors are located close to the epidermal junction or in the dermis [33-34].

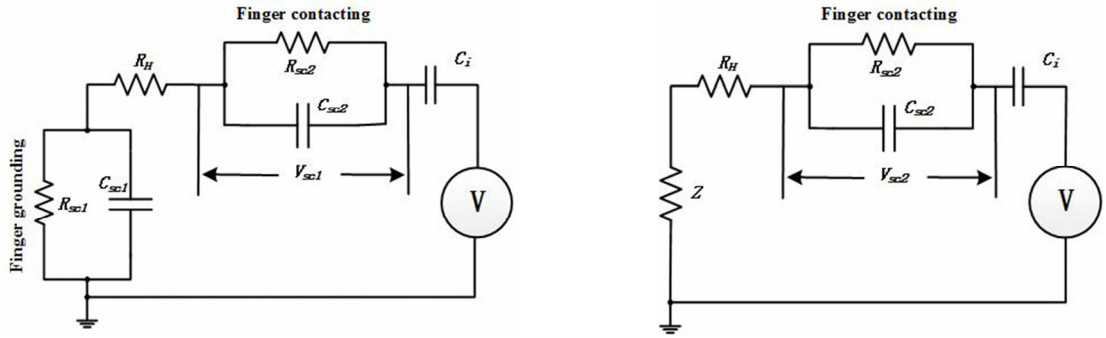

(a) under direct ground connection (b) under nature ground connection

Fig. 3. Equivalent models of electrostatic tactile system

The electrostatic device uses ITO conductive glass and silicon dioxide as the conductor and insulator. The thickness of insulator T_i and stratum corneum T_{sc} are respectively 1μm and 200μm, contact area A is 1cm^2, the vacuum permittivity ε_0 is 8.85 × 10^{-12} F/m, the insulator permittivity is ε_i=3.9, so insulator capacitance C_i can be calculated to 1.35nF [35]. Electrical characteristics of stratum corneum (mainly includes resistance R_{sc} and capacitance C_{sc}) decreases with frequency and can be calculated from (3) and (4). As shown in paper [30] that ε_{sc} and ρ_{sc} vary respectively in the range of 2 × 10^3-10^4 and 4 × 10^4-10^5 in the range of 10Hz-1000Hz, so C_{sc} and R_{sc} are calculated respectively to 44.25nF, 22nF, 8.85nF and 200kΩ, 160kΩ, 80kΩ at 10Hz, 100Hz and 1000Hz [30].

$$C = \frac{\varepsilon_0 \varepsilon_r A}{T} \tag{3}$$

$$R = \frac{\rho T}{A} \tag{4}$$

Based on the voltage dividing effect, we relate V_{sc1} and V_{sc2} to V as shown in (5) and (6), where Z_{sc1}, and Z_{sc2} are respectively stratum corneum impedance of grounding finger and touching finger, $Z_{dir\text{-}total}$ and $Z_{nat\text{-}total}$ are total impedances under direct ground connection and nature ground connection. We establish circuit vector models and obtain amplitude- frequency relationship of C_i, Z_{sc1}, and Z_{sc2}, as shown in (7)-(9). Then, we substitute all parameters into formula and obtain C_i=2.3MΩ and Z_{sc1}=Z_{sc2}=65.7kΩ at 100Hz. It is said in paper [33] that Z is approximately 14.5MΩ when the device is under nature ground connection.

$$V_{sc1} = \frac{Z_{sc2}}{Z_{sc2} + C_i + R_H + Z_{sc1}} V = \frac{Z_{sc2}}{Z_{dir-total}} V \tag{5}$$

$$V_{sc2} = \frac{Z_{sc2}}{Z_{sc2} + C_i + Z} V = \frac{Z_{sc2}}{Z_{nat-total}} V \tag{6}$$

$$\left|\mathrm{C}_i\right| = \left|\frac{1}{j\omega C_i}\right| = \sqrt{\frac{1}{\omega^2 C_i^2}} \tag{7}$$

$$\left|Z_{sc1}\right| = \left|\frac{R_{sc1} \cdot \frac{1}{j\omega \mathrm{C}_{\mathrm{sc1}}}}{R_{sc1} + \frac{1}{j\omega \mathrm{C}_{\mathrm{sc1}}}}\right| = \left|\frac{R_{sc1}}{1 + j\omega R_{sc1} \mathrm{C}_{\mathrm{sc1}}}\right| = \frac{R_{sc1}}{\sqrt{1 + (\omega R_{sc1} \mathrm{C}_{\mathrm{sc1}})^2}} \tag{8}$$

$$\left|Z_{sc2}\right| = \left|\frac{R_{sc2}}{1 + j\omega R_{sc2} \mathrm{C}_{\mathrm{sc2}}}\right| = \frac{R_{sc2}}{\sqrt{1 + (\omega R_{sc2} \mathrm{C}_{\mathrm{sc2}})^2}} \tag{9}$$

As the simulation result of V_{sc1} and V_{sc2} shown in Fig. 4, the output voltage of V_{sc1} is six times larger than that of V_{sc2} because $Z_{dir\text{-}total}$ is much larger than $Z_{nat\text{-}total}$. From (1) we can see that V_{sc2} generates smaller electrostatic force under nature ground connection than that under direct ground connection, causing the non-uniform perceived electrostatic tactile. Therefore, it is necessary for electrostatic tactile system to ground directly to improve effective voltage amplitude and tactile perception.

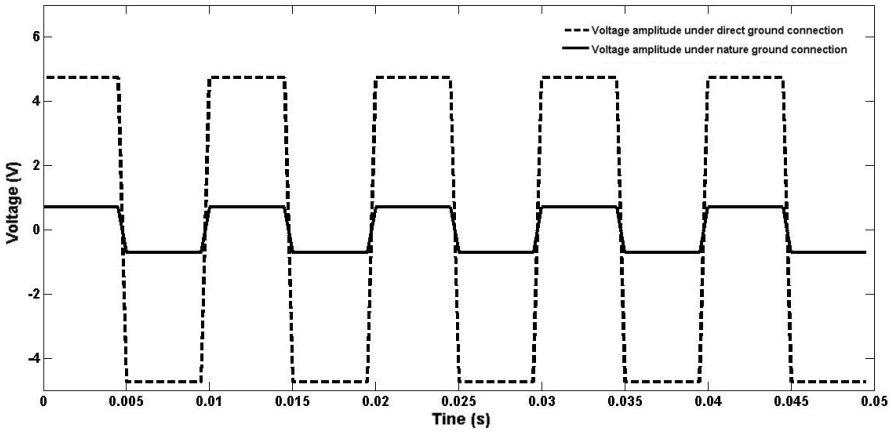

Fig. 4. Comparison of direct grounding and nature grounding

3.2 Human Grounding Points

In this subsection, we explore the effect of human body grounding position based on the equivalent model. When considering grounding methods, antistatic wristbands and device shells are the most used electrodes. When use antistatic wristbands, R_{sc1} and C_{sc1} are the stratum corneum of our wrist, and when hold the metal shell of the mobile devices, R_{sc1} and C_{sc1} are the stratum corneum of our fingertip. Fortunately, human body grounding position must be located in one part of users' body, so we first vary R_{sc1} and C_{sc1} in their ranges to see changes of effective voltage V_{sc1} through circuit simulation software CST.

We first fix C_{sc1} to 22nF and select five equidistant R_{sc1} including 80kΩ, 110kΩ, 140kΩ, 170kΩ and 200kΩ. The partial enlarged views of circuit simulation results of V_{sc1} are shown in Fig. 5, where we use red line with circle, green line with square, purple line with triangle, brown line with asterisk and black line with star to respectively express R_{sc1}=80kΩ, 110kΩ, 140kΩ, 170kΩ and 200kΩ. Similarly, we then fix R_{sc1} to 160$k\Omega$ and select five equidistant C_{sc1} including 8.85nF, 17.7nF, 26.5nF, 35.4nF and 44.2nF, as shown in Fig. 6. The global views are also provided to show the integral trends. The applied voltage we used is bipolar square wave with the peak-to-peak amplitude of 360V and the frequency of 100Hz.

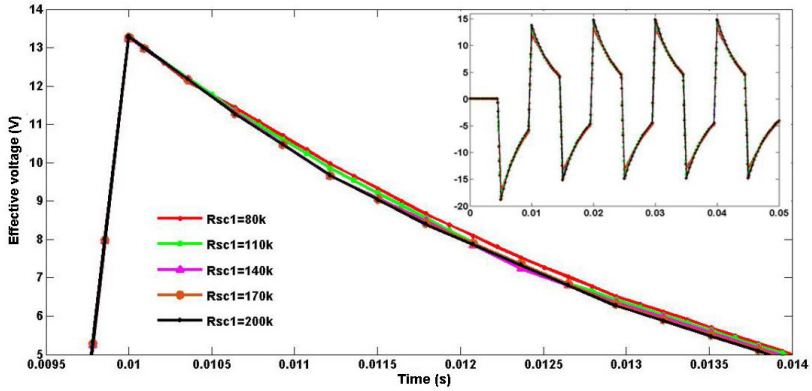

Fig. 5. Simulation results with varying R_{sc1} and fixed C_{sc1}

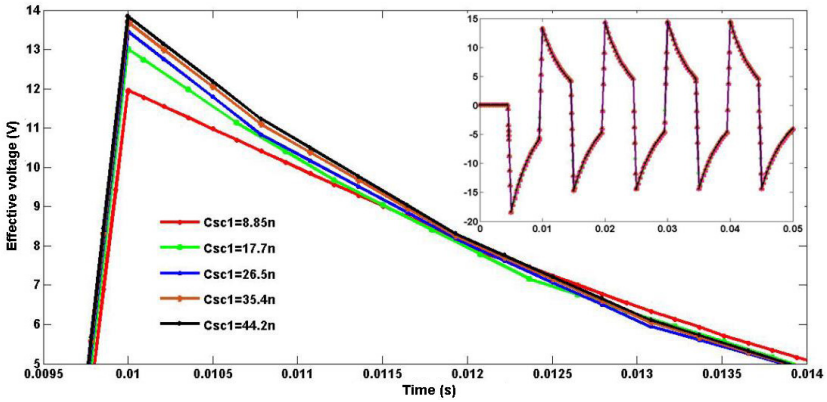

Fig. 6. Simulation results with varying R_{sc1} and fixed C_{sc1}

As the simulation result with varying R_{sc1} and fixed C_{sc1} shown in Fig. 5, R_{sc1} result in some little effect in the voltage dropping process but not at the peak voltage. The effect of different R_{sc1} on V_{sc1} is too small to result in tactile perceived difference, so we can ignore the effect of R_{sc1} when establishing the system model.

As the simulation result with varying C_{sc1} and fixed R_{sc1} shown in Fig. 6, C_{sc1} result in an impact at the peak voltage but not in the voltage dropping process. The effective voltage V_{sc1} under smaller C_{sc1} is significantly larger than that of bigger one in same R_{sc1}. The voltage difference reaches up to 2V with the maximum voltage 13.84V in case of C_{sc1}=8.85nF and the minimum voltage 11.96V in case of C_{sc1}=44.2nF, so we can conclude that the effect of different grounding parts mainly comes from skin

capacitance. Only few people own the two extreme C_{sc1} and affected by C_{sc1}, so we conclude that different human body grounding position have not effect on electrostatic tactile system for most people.

3.3 Human Impedance

Because the effect of different human body grounding position is too small to detect, human body grounding position can be placed in any positions in practical usage. To simplify the system equivalent model, we assume that human body grounding position have the same skin characteristics as the sliding points and then equivalent the electrostatic tactile system to the simplified model shown as Fig. 7, where R_{sc} and C_{sc} are skin impedances in sliding finger.

In this subsection, we first convert the complicated circuit mixed series and parallel connection into simple series connection. As shown in Fig. 8, human body can be equivalent to series and parallel connection of skin resistance R_{sc}, skin capacitance C_{sc} and human impedance R_H. Human impedance R_H is usually less than 1kΩ and determined as 500Ω by H. Freiberger [36]. Skin characteristics R_{sc} and C_{sc} vary in the range of 80kΩ-200kΩ and 8.85nF-44.25nF at low frequency.

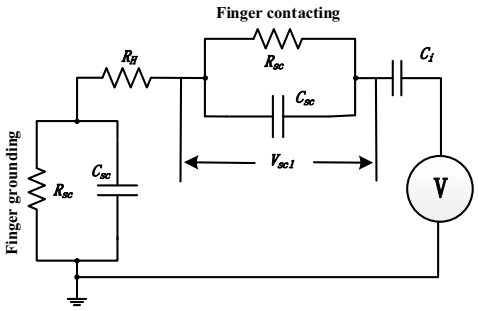

Fig. 7. Simplified equivalent model of electrostatic system

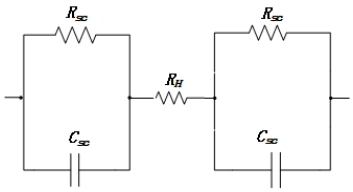

Fig. 8. Equivalent model of human body by H. Freiberger

The parallel-equivalent model of human skin can be derived to series-equivalent model by using equivalent transformation method. The parallel-equivalent impedance R_{sc} and C_{sc} can be equivalent to the series-equivalent resistance R_x and reactance X_x through (10)-(12), where f is frequency, $w=2\pi f$ is angular frequency, $X_x = 1/wC_x$ and $X_{sc} = 1/wC_{sc}$ are respectively impedances of C_x and C_{sc}. The series-equivalent capacitance C_x can be obtained from (10) and (12), as shown in (13).

$$R_x + jX_x = \frac{R_{sc}(jX_{sc})^2}{R_{sc}^2 + X_{sc}^2} + j\frac{R_{sc}^2 X_{sc}}{R_{sc}^2 + X_{sc}^2} \tag{10}$$

$$R_x = \frac{R_{sc}X_{sc}^2}{R_{sc}^2 + X_{sc}^2} = \frac{R_{sc}}{1+(wC_{sc}R_{sc})^2} \tag{11}$$

$$X_x = \frac{R_{sc}^2 X_{sc}}{R_{sc}^2 + X_{sc}^2} = \frac{w\mathrm{C_{sc}}R_{sc}^2}{1+(w\mathrm{C_{sc}}R_{sc})^2} \tag{12}$$

$$C_x = \frac{1+(wC_{sc}R_{sc})^2}{(wR_{sc})^2 \cdot C_{sc}} \tag{13}$$

Based on above method, we simplify the human body model to the series-equivalent model shown in Fig. 9, where R_x and C_x are derived from R_{sc} and C_{sc}, $R_{x'}$ and $C_{x'}$ are the final equivalent of skin resistance and capacitance. We choose R_{sc}=160kΩ and C_{sc}=22nF at 100Hz to calculate resistance and capacitance in series-equivalent model to R_x=27.16kΩ and C_x=26.5nF respectively. There we choose stratum corneum characteristics at 100Hz because they are median values in their frequency ranges.

(a) parallel combinations (b) equivalent series combinations

Fig. 9. Equivalent transformation of a resistor and capacitor

Finally, we calculate the final-equivalent resistance $R_{x'}$ to 54.32kΩ from (14), which is far more than human impedance R_H.

$$R_{x'}=\frac{2R_{sc}}{1+(2\pi f\,\mathrm{C_{sc}}\,R_{sc})^2} \tag{14}$$

To explore the effect of human impedance R_H, we introduce the quality factor Q to compare the output difference with and without R_H. Q is a quality index of the syntonic circuit which is defined as the ratio of the stored energy and the lost energy in one cycle. The calculation method of Q in series structure is equal to that of parallel structure, as shown in (15). The quality factor with human impedance Q_{with} approaches that without human impedance $Q_{without}$, as shown in (16) and (17), where $C_{x'}$ is calculated to 13.25nF. There is only about 0.909% difference between the models with and without R_H.

$$Q=\frac{X_x}{R_x}\ \text{(series model)}=\frac{R_{sc}}{X_{sc}}\ \text{(parallel model)} \tag{15}$$

$$Q_{with}=\frac{X_{x'}}{R_{x'}+R_H}=\frac{1}{wC_{x'}\cdot(R_{x'}+R_H)}=2.1911 \tag{16}$$

$$Q_{without}=\frac{X_{x'}}{R_{x'}}=\frac{1}{wC_{x'}R_{x'}}=2.2112 \tag{17}$$

In addition, we built circuit simulation models with/without R_H through circuit simulation software CST to show the effect of R_H on effective voltage V_{sc1}. The applied voltage we used is bipolar square wave with the peak-to-peak amplitude of 360V and the frequency of 100Hz. The simulation result is shown in Fig. 10. V_{sc1} with human impedance shown in the blue line with square marks is extremely close to that without human impedance shown in the red line with circular marks, illustrating that the difference caused by R_H is too small to have an effect. Therefore, we conclude from impedance comparison result, quality factor comparison result and circuit simulation result that the effect of human impedance on electrostatic tactile system can be neglected. In the next narration, we will remove human impedance R_H from electrostatic tactile system equivalent model.

Because the effect of human impedance is too small to detect, we take the human impedance out and simplify the system equivalent to make it more practical, as shown in Fig. 11.

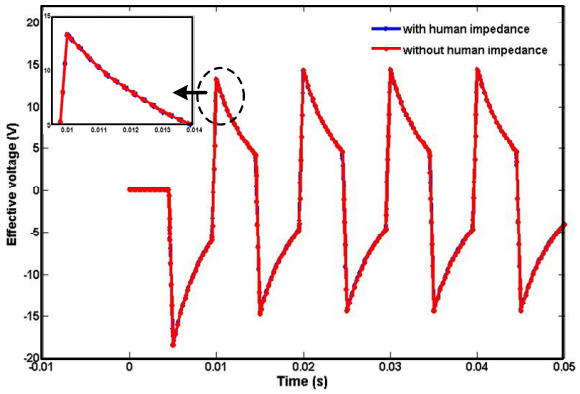

Fig. 10. Effective voltage with/without R_H

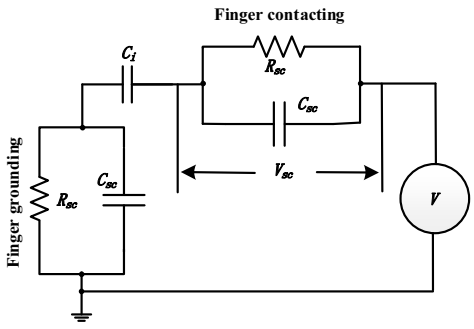

Fig. 11. Final equivalent model of electrostatic tactile system

3.4 Insulator Capacitance

Based on the electrostatic tactile system model, we explore the effect of insulator capacitance in this subsection. The capacitance value of the insulator determines what kind of material Electrostatic tactile devices used as tactile screen to represent tactile. As shown in (3), C_i is affected by ε_i and T_i when assuming ε_0 and A as two constants. As shown in (1), ε_i and T_i affects the electrostatic force directly. In addition, we can easily see that ε_i and T_i affect the effective output voltage too. Therefore, we must consider the effects of ε_i and T_i on the numerator and denominator of the electrostatic force at the same time.

To solve above problem, we use MATLAB to simulate the electrostatic force in two cases: One is fixed T_i and varying ε_i from 1 to 10, the other is fixed ε_i and varying T_i from 0.01μm to 10μm. To show the variation trend of the force, we use normalized y-axis. As the ε_i simulation results shown in Fig. 13, the electrostatic force increases approximately linearly with the increase of ε_i and decreases with the increase of T_i. The force increased trend of ε_i is approximately linear, whereas that of T_i decreases sharply from 0 to 1μm and reaches almost 0 after 0.2μm. From simulation we can see that larger ε_i and smaller T_i, in other words larger C_i can cause larger electrostatic force and better represented effect. It should be pointed out that smaller T_i may be bring the problem of poor insulator, but this is out of the scope of this paper.

Our screen uses 3M Microsoft panel to represent tactile due to the advantages of high integration, small volume and heuristics usability. Its parameters are shown in the dots of Fig. 12. Developing better materials is of great importance to improve the representation performance of Electrostatic tactile device.

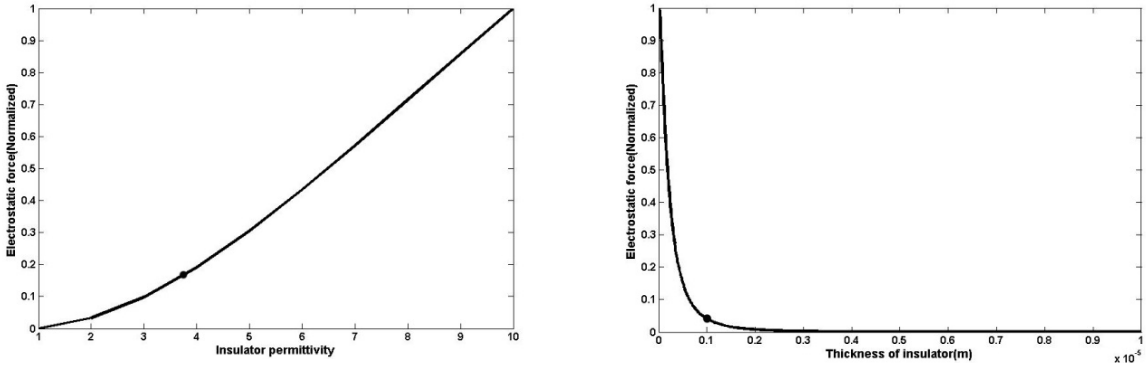

(a) effect of ε_i (b) effect of T_i

Fig. 12. Effect of insulator capacitance on the electrostatic force

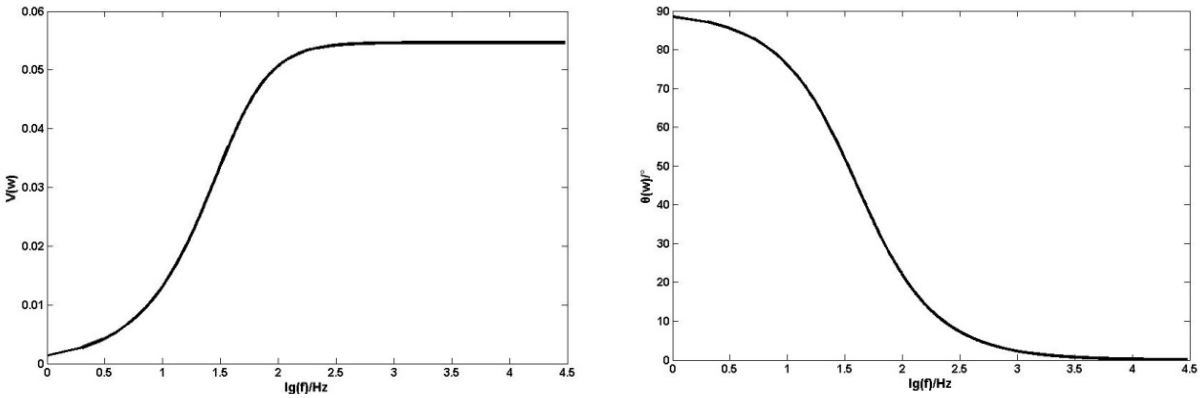

(a) Amplitude-frequency characteristic (b) Phase-frequency characteristic

Fig. 13. System frequency characteristics in the whole working bandwidth

4 System Characteristics Analysis

4.1 Frequency Characteristics

We calculate the applied voltage V and the effective voltage V_{sc} using electrical circuit theory, as shown in (18)-(21), where jw is the Fourier transform variable, $I(jw)$ is the assumed trunk current, $V_{sc}(jw)$ and $V(jw)$ are the system output voltage and input voltage in the frequency domain. The system function $H(jw)$ which is defined as the ratio of system output and system input is used to analyze the system frequency characteristic. After that, we obtain $V_{sc}(t)$ through inverse Fourier transformation and introduce $V_{sc}(t)$ to (1) to obtain electrostatic force $f_e(t)$ shown in (22) and friction force $f(t)$ shown in (2).

$$V(jw) = [\frac{2R_{sc}}{1 + sR_{sc}\,\mathrm{C_{sc}}} + \frac{1}{sC_i}] \cdot I(jw) \tag{18}$$

$$V_{sc}(jw) = \frac{R_{sc}}{1 + sR_{sc}\,\mathrm{C_{sc}}} \cdot I(jw) \tag{19}$$

$$V_{sc}(jw) = \frac{jw \cdot R_{sc}C_i}{jw \cdot (2R_{sc}C_i + \mathrm{C_{sc}}\,R_{sc}) + 1} V(jw) \tag{20}$$

$$H(jw) = \frac{V_{sc}(jw)}{V(jw)} = \frac{jw \cdot R_{sc}C_i}{jw \cdot (2R_{sc}C_i + \mathrm{C_{sc}}\,R_{sc}) + 1} \tag{21}$$

$$f_e(t) = \frac{\varepsilon_0 A V_{sc}^2(t)}{2(\frac{T_i}{\varepsilon_i} + \frac{T_{sc}}{\varepsilon_{sc}})(T_{sc} + T_i)} \tag{22}$$

To simplify the calculation, we use a and b to express $R_{sc}C_i$ and $2R_{sc}C_i+R_{sc}C_{sc}$. The real part R_e and imaginary part I_m of the system function shown in (24) are calculated from (23). Then, we calculate the amplitude-frequency characteristic defined as the square root of $R_e^2+I_m^2$ and the phase-frequency characteristic defined as the arctangent of the ratio of R_e and I_m, as shown in (25) and (26).

$$H(jw) = \frac{abw^2 + jwa}{1 + (wb)^2} \tag{23}$$

$$R_e = \frac{abw^2}{1 + b^2w^2};\ I_m = \frac{aw}{1 + b^2w^2} \tag{24}$$

$$V(w) = \sqrt{R_e^{\,2} + I_m^{\,2}} = \sqrt{\frac{a^2w^2}{1 + b^2w^2}} \tag{25}$$

$$\theta(w) = arctan(\frac{I_m}{R_e}) = arctan(\frac{1}{bw}) \tag{26}$$

As the simulation results of the system frequency characteristics shown in Fig. 13, the electrostatic system can be seen as a first order high-pass filter in the whole working bandwidth. The frequency characteristics are also simulated in 10Hz-1000Hz which is the range of human perceptible frequency bandwidth, as shown in Fig. 14. The knee frequency and steady frequency of the amplitude-frequency characteristic are roughly calculated as 40Hz and 300Hz, which means that the attenuation of input signals are getting worse in the range of 10Hz-40Hz, gradually getting better in the range of 40Hz-300Hz and disappeared after 300Hz. The attenuation more serious, the output signals become smaller, resulting weaker tactile in users' fingers and causing worse representation effects. The knee frequency and steady

frequency of the phase-frequency characteristic are roughly calculated as 90Hz and 270Hz, which means that the phase-shift problem of the input signals are getting worse, gradually getting better and disappeared respectively in the range of 10Hz-90Hz, 90Hz-270Hz and after 270Hz. The phase-shift problem more serious, the phase offset of output signals larger, the difference between input signal and output signal larger, resulting more inauthentic tactile.

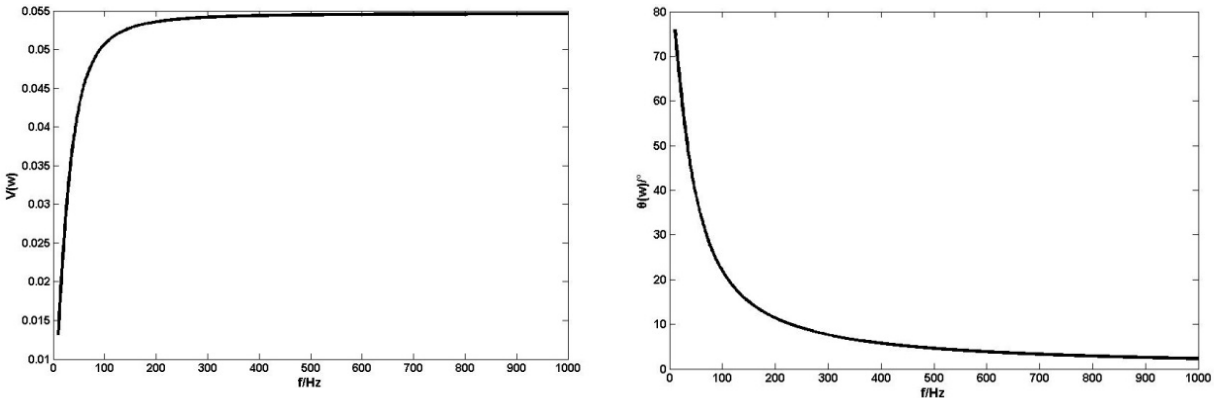

(a) Amplitude-frequency characteristic in 10-1000Hz (b) Phase-frequency characteristic in 10-1000Hz

Fig. 14. System frequency characteristics in 10-1000Hz

We can see the best applied frequency range which is of great importance in designing applications of electrostatic tactile system in simulation results of amplitude & phase-frequency characteristics:

(1) To avoid attenuation of the signal amplitude, the input signals should not be less than 40Hz. The range of 300Hz-1000Hz should be given priority and then the range of 40Hz-300Hz in the multi-level perceptive applications such as when using different feelings to represent different fruits in Fruit Ninja game or different plants in Plants vs. Zombies game;

(2) To avoid phase-shift of the signal, the input signals should not be less than 90Hz. The range of 270Hz-1000Hz should be given priority and then the range of 90Hz-270Hz. Taking the effects of signal amplitude and phase into account, the input signals should not be less than 90Hz and the range of 300Hz-1000Hz should be given priority when designing Electrostatic tactile applications.

4.2 Waveform Characteristic

Three common bipolar waveforms with Vpp=30V and f=100Hz, sinusoidal wave, triangular wave and square wave, are used to explore the effect of waveforms on system output. The effect cannot be studied directly in the time domain from (1), so we consider to analyze it in the frequency domain through the system function: We first calculate the Fourier transformation of input signals $V(jw)$ and then obtain the system output signals $V_{sc}(jw)$ through multiplying $V(jw)$ with the system function. Finally, we calculate the time domain output signals $V_{sc}(t)$ through inverse Fourier transformation.

The simulation results are shown in Fig. 15, where top half of three subgraphs are the applied signals and the bottom half are the output signals. To simplify the narrative, we use V_{sin}, V_{tri}, V_{squ} and V_{sinsc}, V_{trisc}, V_{squsc} to express three different applied signals and output signals respectively. The output signals have the same frequency as the input signals, whereas the amplitude and the shape have significant difference:

(1) V_{sinsc} has the same shape as V_{sin}, whereas V_{trisc} and V_{squsc} have a certain degree of waveform change compared with V_{tri} and V_{squ}. From the sharpness of waveforms, V_{trisc} is shaper than V_{sinsc};

(2) The amplitudes of all output signals are significantly smaller than input signals, and square wave has larger amplitude than other two waves. From the peak-to-peak value of output signals, V_{squsc} has the largest value of almost 30V, whereas V_{sinsc} and V_{trisc} have almost 15V.

The study of waveform characteristic has an important significance in expanding the available signal range and improving tactile experience:

(1) Voltage difference plays a leading role in representing tactile, so square wave can generate strongest feeling than others because of its largest voltage difference;

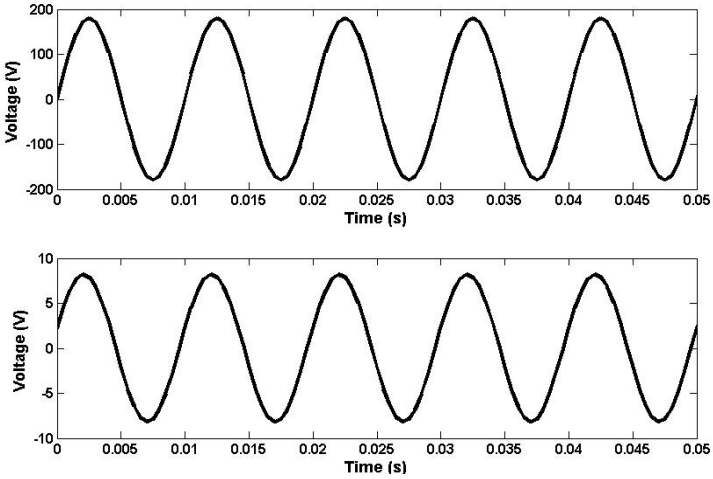

(a) Sinusoidal wave

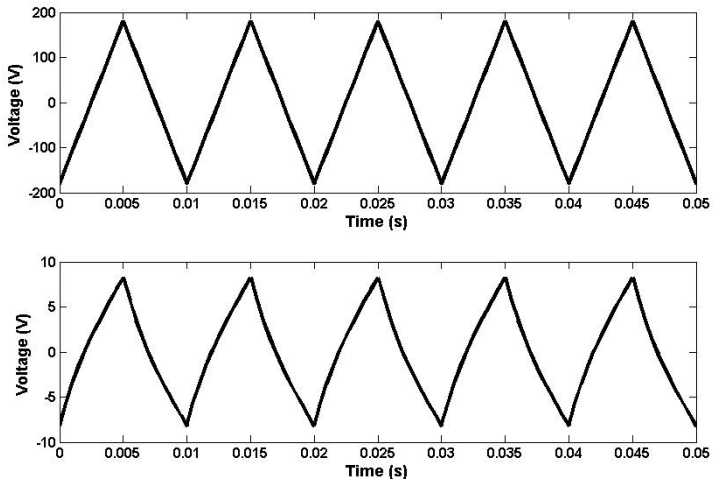

(b) Triangular wave

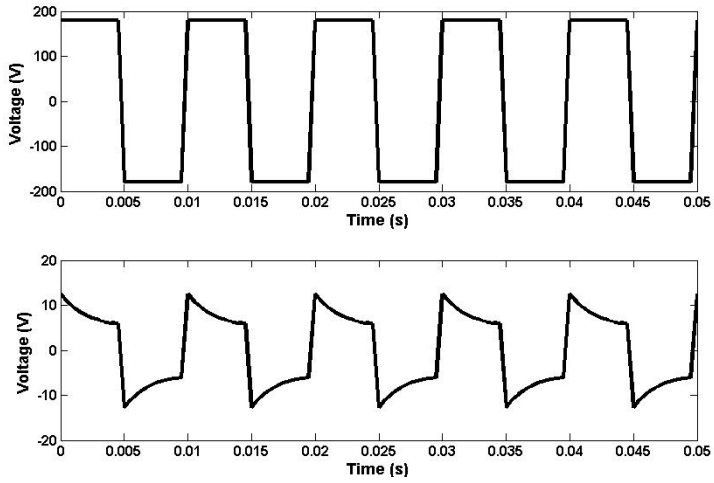

(c) Square wave

Fig. 15. System waveform characteristics

(2) Sinusoidal wave and triangular wave generate weaker feelings than square wave. The feeling of sinusoidal wave is smooth and "soft", whereas that of triangular wave is shape and rough, so triangular wave may feel stronger than sinusoidal wave.

5 Conclusion and Future Work

With a custom-designed electrostatic tactile device, we studied the effects of four factors, ground connection method, human body grounding position, human impedance, insulator capacitance, on tactile representation performance of electrostatic tactile system. All these analysis are of great importance in establishing effective equivalent circuit model of the electrostatic tactile system and improving system representation performance greatly. Analysis results show that we must take the effect of ground connection method into account, but the effect of human body grounding position and human impedance can be ignored, illustrating that electrostatic tactile devices can be used by most different kinds of people with grounding points setting into any positions. We also show that larger permittivity and smaller thickness of insulator cause better system performance, guiding the future selection of system tactile representation materials. The presented model in this paper can be used in future researches to design more applications to enhance user experience of the existing touch screen devices.

In the future, more factors including the environmental factors and the human factors will be considered and explored to establish more accuracy models. We will also study the mismatches to find their reason and try to avoid. In addition, the appropriate position prediction algorithms of finger positioning technology will be studied too.

Acknowledgements

This work was supported by the National Natural Science Foundation of China (61631010).

References

[1] O. Bau, I. Poupyrev, A. Israr, TeslaTouch: electrovibration for touch surfaces, in: Proc. 2010 Annual ACM Symposium on User Interface Software and Technology, 2010.

[2] S. Brewster, F. Chohan, L. Brown, Tactile feedback for mobile interactions, in: Proc. 2007 the SIGCHI Conference on Human Factors in Computing Systems, 2007.

[3] K. Yatani, K.N. Truong, SemFeel: a user interface with semantic tactile feedback for mobile touch-screen devices, in: Proc. 2009 Annual ACM Symposium on User Interface Software and Technology, 2009.

[4] G.H. Yang, M. Jin, Y. Jin, T-mobile: vibrotactile display pad with spatial and directional information for hand-held device, in: Proc. 2010 IEEE/RSJ International Conference on Intelligent Robots and Systems (IROS), 2010.

[5] N. Asamura, N. Tomori, H. Shinoda, A tactile feeling display based on selective stimulation to skin receptors, in: Proc. 1998 Virtual Reality Annual International Symposium, 1998.

[6] N. Asamura, N. Yokoyama, H. Shinoda, Selectively stimulating skin receptors for tactile display, IEEE Computer Graphics & Applications 18(6)(1998) 32-37.

[7] L. Winfield, J. Glassmire, J.E. Colgate, T-pad: tactile pattern display through variable friction reduction, in: Proc. 2007 Joint EuroHaptics Conference and Symposium on Haptic Interfaces for Virtual Environment and Teleoperator Systems, 2007.

[8] N.D. Marchuk, J.E. Colgate, M.A. Peshkin, Friction measurements on a Large Area TPaD, in: Proc. 2010 Haptics Symposium, 2010.

[9] X. Dai, J Gu, X. Cao, SlickFeel: sliding and clicking haptic feedback on a touchscreen, in: Proc. 2012 Annual ACM Symposium on User Interface Software and Technology, 2012.

[10] K.A. Kaczmarek, K. Nammi, A.K. Agarwal, M.E. Tyler, S.J. Haase, D.J. Beebe, Polarity effect in electrovibration for tactile display, IEEE Transactions on Biomedical Engineering 50(10)(2006) 2047-2054.

[11] A. Yamamoto, S. Nagasawa, H. Yamamoto, T. Higuchi, Electrostatic tactile display with thin film slider and its application to the tactile telepresentation systems, IEEE Trans. Visualization and Computer Graphics 12(2)(2006) 168-177.

[12] O. Bau, I. Poupyrev, REVEL: tactile feedback technology for augmented reality, Acm Transactions on Graphics 31(4)(2012) 1-11.

[13] S.C. Kim, A. Israr, I. Poupyrev, Tactile rendering of 3D features on touch surfaces, in: Proc. 2013 Annual ACM Symposium on User Interface Software and Technology, 2013.

[14] T. Wang, X. Sun, Electrostatic tactile rendering of image based on shape from shading, in: Proc. 2014 International Conference on Audio, Language and Image Processing, 2014.

[15] S. Wu, X. Sun, Q. Wang, J. Chen, Tactile modeling and rendering image-textures based on electrovibration, The Visual Computer 33(5)(2016) 637-646.

[16] G. Ilkhani, M. Aziziaghdam, E. Samur, Data-driven texture rendering with electrostatic attraction, Springer Berlin Heidelberg, Berlin,496-504.

[17] D.J. Meyer, Electrostatic force on a human fingertip, [dissertation] Evanston, IL: Northwestern University, 2012.

[18] D.J. Meyer, M.A. Peshkin, J.E. Colgate, Fingertip friction modulation due to electrostatic attraction, in: Proc. 2013 World Haptics Conference, 2013.

[19] F. Giraud, M. Amberg, B.L. Semail, Merging two tactile stimulation principles: electrovibration and squeeze film effect, in: Proc. 2013 World Haptics Conference, 2013.

[20] E. Vezzoli, M. Amberg, F. Giraud, B. Lemaire-Semail, Electrovibration modeling analysis, in: M. Auvray, C. Duriez (eds.), EUROHAPTICS, Springer Berlin Heidelberg, 2014, pp. 369-376.

[21] Y. Tanaka, T. Onishi, Tsuji T, N. Yamada, Y. Takeda, I. Masamori, Analysis and modeling of human impedance properties for designing a human-machine control system, in: Proc. 2007 IEEE International Conference on Robotics and Automation, 2007.

[22] R.M. Strong, D.E. Troxel, An electrotactile display, IEEE Trans. Man-Machine Systems1(11)(1970) 72-79.

[23] C. Xu, A. Israr, I. Poupyrev, O. Bau, C. Harrison, Tactile display for the visually impaired using TeslaTouch, in: Proc. 2011 CHI ’11 Extended Abstracts on Human Factors in Computing Systems, 2011.

[24] A. Israr, O. Bau, S.C. Kim, I. Poupyrev, Tactile feedback on flat surfaces for the visually impaired, in: Proc. 2012 CHI ’12 Extended Abstracts on Human Factors in Computing Systems, 2012.

[25] D.J. Meyer, M. Wiertlewski, M.A. Peshkin, J.E. Colgate, Dynamics of ultrasonic and electrostatic friction modulation for rendering texture on haptic surfaces, in: Proc. 2014 Haptics Symposium (HAPTICS), 2014.

[26] E. Vezzoli, W.B. Messaoud, M. Amberg, F. Giraud, B.L. Semail, M.A. Bueno, Physical and perceptual independence of ultrasonic vibration and electrovibration for friction modulation, IEEE Transactions on Haptics 8(2)(2015) 235-239.

[27] H. Kim, J. Kang, K.D. Kim, K.M. Lim, J. Ryu, Method for providing electrovibration with uniform intensity, IEEE Transactions on Haptics 8(4)(2015) 492-496.

[28] Y. Vardar, B. Güçlü, C. Basdogan, Effect of waveform in haptic perception of electrovibration on touchscreens, in: Proc. 2016 International Conference on Haptics: Perception, Devices, Control, and Applications, 2016.

[29] H. Fruhstorfer, U. Abel, C.D. Garthe, Thickness of the stratum corneum of the volar fingertips, Clinical Anatomy 13(6)(2000) 429-433.

[30] T. Yamamoto, Y. Yamamoto, Dielectric constant and resistivity of epidermal stratum corneum, Medical and Biological Engineering and Computing 14(5)(1976) 494-500.

[31] T. Yamamoto, Y. Yamamoto, Electrical properties of the epidermal stratum corneum, Medical and Biological Engineering 14(2)(1976) 151-158.

[32] C.D. Shultz, M.A. Peshkin, J.E. Colgate, Surface haptics via electroadhesion: expanding electrovibration with Johnsen and Rahbek, in: Proc. 2015 World Haptics Conference, 2015.

[33] Y. Vardar, B. Guclu, C. Basdogan, Effect of waveform on tactile perception by electrovibration displayed on touch screens, IEEE Transactions on Haptics PP(99)(2017) 1-1.

[34] B. Güçlü, S.J. Bolanowski, L. Pawson, End-to-end linkage (EEL) clustering algorithm: a study on the distribution of Meissner corpuscles in the skin, Journal of Computational Neuroscience 15(1)(2003) 19-28.

[35] H. Fruhstorfer, U. Abel, C.D. Garthe, A. Knüttel, Thickness of the stratum corneum of the volar fingertips, Clinical Anatomy 13(6)(2000) 492-433.

[36] C.J. Poletto, C.L. V. Doren, A high voltage, constant current stimulator for electrocutaneous stimulation through small electrodes, IEEE Trans. Biomedical Engineering 46(8)(1999) 929-936.